

# Adaptive Choice of Process Noise Covariance in Kalman Filter Using Measurement Matrices

Yoji Takayama<sup>1</sup>, Takateru Urakubo<sup>1</sup>, Member, IEEE, and Hisashi Tamaki, Member, IEEE

**Abstract**—For the systems working in unknown environments, the number and quality of measurements may vary depending on the environment. In the Kalman filter, it is common to add fictitious noises to the nominal process and measurement noises to avoid the filter divergence caused by inaccurate system modeling. However, it is difficult to choose an appropriate fictitious noise, especially for the systems whose environment varies with respect to the measurements. A naively chosen fictitious noise often leads to unexpectedly large inflation of state estimation error covariance and even degradation of estimation accuracy, when the number of measurements is less than the number of states. This article proposes a novel method for adding a fictitious noise to the nominal process noise using the measurement matrix at each time step. First, we analyze theoretically the variations of state estimation error covariance and Kalman gain due to a fictitious noise. Next, based on the results, we seek a fictitious noise that minimizes the expected values of measurement residuals at each time step and show that unnecessary inflation of state estimation error covariance can be avoided by choosing the fictitious noise based on the measurement matrix. Experiments on positioning of actual automobiles using global navigation satellite system (GNSS) and inertial navigation system (INS) demonstrate that the proposed method improves the positioning accuracy compared to conventional methods. The proposed method has a novel feature in that it is not adaptive to the measurements themselves, but to the measurement matrix, and can be applied in a computationally effective manner to practical applications.

**Index Terms**—Adaptive filter, extended Kalman filter (EKF), filter divergence, sensitivity analysis.

## I. INTRODUCTION

AUTONOMOUS systems in outdoor environments such as mobile electronic devices, mobile robots, and self-driving cars are becoming more widespread. Although many sensors are mounted in the systems to detect their own position, surrounding obstacles, landmarks, and so on, the number of available sensors and the quality of measurement data would vary drastically depending on the environment where the systems are working. For example, when global navigation satellite system (GNSS) positioning is performed in urban canyons, the number of visible satellites becomes quite few,

Manuscript received 19 December 2022; revised 6 November 2023; accepted 23 November 2023. Date of publication 14 December 2023; date of current version 25 April 2024. Recommended by Associate Editor Y. Yildiz. (Corresponding author: Yoji Takayama.)

Yoji Takayama is with Furuno Electric Company Ltd., Nishinomiya, Hyogo 662-8580, Japan (e-mail: yohji.takayama.kh@furuno.co.jp).

Takateru Urakubo and Hisashi Tamaki are with the Department of System Informatics, Graduate School of System Informatics, Kobe University, Kobe, Hyogo 657-8501, Japan (e-mail: t.urakubo@silver.kobe-u.ac.jp; tamaki@al.cs.kobe-u.ac.jp).

Digital Object Identifier 10.1109/TCST.2023.3339732

and their geometrical distribution can be biased. For a mobile robot with LiDAR, if there are a small number of objects in the measurement range, only a few beams can provide information on the robot's position. Also, when the robot moves along a flat wall, the information from LiDAR would degenerate [1], [2].

The Kalman filter is a powerful tool for estimating the state of a system by combining a lot of measurements with a mathematical model of the system [3], [4]. Since many actual systems cannot be exactly represented by a linear system model, we use the extended Kalman filter (EKF), unscented Kalman filter, and other filters on the understanding that there will exist some model error. However, the inaccurate model often leads to unexpectedly large estimation errors and further filter divergence.

For systems with inaccurate models, many approaches have been proposed so far to mitigate the increase in estimation errors or to avoid the filter divergence by choosing appropriately the covariances of process noise and measurement noise in the filters. A common heuristic approach is to add fictitious noises to the nominal noise covariances of the original system model. Because of the fictitious noises for process noise and measurement noise, the covariance of state estimation error in the filter becomes sufficiently large to cover the model error, and the filter divergence is avoided. Although the fictitious noises are often given by trial and error, naively chosen fictitious noises tend to unintentionally inflate the state estimation error covariance and result in degraded estimation accuracy, especially for the systems where the number of measurements is less than the number of state variables, as we pointed out in [5] and [6]. A fading memory filter (FMF) can be viewed as one of the fictitious noise approaches. By weighting the estimation errors according to their time steps, FMF takes more account of the recent estimation error, which is equivalent to the process noise covariance being increased by a certain fictitious noise. Even when FMF is employed, the degradation of estimation accuracy with the unintentional inflation of estimation error covariance has been reported in [7], [8], [9], and [4].

Another common approach is to adaptively modify the process noise and measurement noise covariances using actual measurements [10], [11], [12]. The appropriate values of the covariances are estimated based on the measurements obtained in multiple steps under the assumption that noise statistics are ergodic. A moving average technique of the measurement covariance has recently been proposed to estimate the process noise covariance using the ergodic property [13]. However, when the noise statistics vary with time steps, it is difficult

to choose how many measurement steps should be used for estimation. In addition, it has been known that the estimation of the process noise covariance matrix cannot be determined uniquely when the number of measurements is less than the number of state variables [14]. Adaptive modeling of the process noise covariance matrix has also been tackled with the help of machine learning approaches in the recent literature [15], [16].

In this article, we propose a novel method to add a fictitious noise to the nominal process noise in EKF based on the measurement matrix at each time step. We analyze the variations of state estimation error covariance and Kalman gain due to a fictitious noise and determine the fictitious noise that minimizes the expected values of measurement residuals at each time step, without assuming the ergodic property. By creating fictitious noise using the measurement matrix that represents the number and quality of measurements, the measurement residuals can be reduced without unnecessary inflation of state estimation error covariance. Although the proposed method can be seen as one of the adaptive choices of process noise covariance, it is not adaptive to the measurements themselves, but to the measurement matrix. In addition, we demonstrate the effectiveness of the proposed method by a numerical example of positioning with LiDAR and an experimental example of positioning with GNSS and inertial navigation system (INS).

The contribution of this article is twofold. First, to the best of our knowledge, the proposed method is the first to choose the process noise covariance adaptively to the measurement matrix to overcome the accuracy degradation caused by an inaccurate model. We call EKF with the proposed method  $H$ -adaptive filter in this article. Second, it is shown that the proposed method works well for a practical application, that is, GNSS/INS positioning of actual automobiles running in outdoor environments where the number and geometric distribution of visible satellites vary largely.

## II. EKF WITH FICTITIOUS NOISE

### A. EKF Overview

We consider a discrete nonlinear system

$$x_k = f(x_{k-1}) + w_k \quad (1)$$

$$y_k = h(x_k) + v_k \quad (2)$$

where the state vector and the measurement vector at time step  $k$  are denoted as  $x_k \in \mathbb{R}^n$  and  $y_k \in \mathbb{R}^m$ , respectively. The process noise and measurement noise are represented by  $w_k \in \mathbb{R}^n$  and  $v_k \in \mathbb{R}^m$ , respectively, and the sequences  $\{w_k\}$  and  $\{v_k\}$  are assumed to be white, zero-mean and uncorrelated with one another. The covariance matrices for  $w_k$  and  $v_k$  are expressed by  $Q_k$  and  $R_k$ , respectively.

Assuming that the functions  $f$  and  $h$  are differentiable as necessary, the system in (1) and (2) can be linearized around a prior estimate  $\hat{x}_k^-$  or a posterior estimate  $\hat{x}_k^+$  as follows:

$$x_k = F_{k-1}x_{k-1} + u_{k-1} + w_k \quad (3)$$

$$\eta_k = H_k x_k + v_k \quad (4)$$

where

$$F_k = \left. \frac{\partial f(x_k)}{\partial x_k} \right|_{x_k=\hat{x}_k^+}, \quad H_k = \left. \frac{\partial h(x_k)}{\partial x_k} \right|_{x_k=\hat{x}_k^-} \quad (5)$$

$$u_k = f(\hat{x}_k^+) - F_k \hat{x}_k^+, \quad \eta_k = y_k - h(\hat{x}_k^-) + H_k \hat{x}_k^-. \quad (6)$$

The EKF for the system in (3) and (4) can be written as follows:

$$\hat{x}_k^- = f(\hat{x}_{k-1}^+) \quad (7)$$

$$P_k^- = F_{k-1} P_{k-1}^+ F_{k-1}^T + Q_k \quad (8)$$

$$\hat{x}_k^+ = \hat{x}_k^- + K_k [y_k - h(\hat{x}_k^-)] \quad (9)$$

$$P_k^+ = (I - K_k H_k) P_k^- \quad (10)$$

$$= (I - K_k H_k) P_k^- (I - K_k H_k)^T + K_k R_k K_k^T \quad (11)$$

$$= \left[ (P_k^-)^{-1} + H_k^T R_k^{-1} H_k \right]^{-1} \quad (12)$$

$$K_k = P_k^- H_k^T (H_k P_k^- H_k^T + R_k)^{-1} \quad (13)$$

$$= P_k^+ H_k^T R_k^{-1} \quad (14)$$

where  $\hat{x}_k$  and  $P_k$  denote, respectively, the state estimate and the estimation error covariance matrix, and  $K_k$  is Kalman gain. The superscripts  $-$  and  $+$  for  $\hat{x}_k$  and  $P_k$  mean “prior” and “posterior.” In (10)–(14),  $P_k^+$  and  $K_k$  are represented in several ways for later use.

We also define estimation errors in  $\hat{x}_k^-$  and  $\hat{x}_k^+$  for convenience of later use as follows:

$$e_k^- \equiv x_k - \hat{x}_k^- \quad (15)$$

$$e_k^+ \equiv x_k - \hat{x}_k^+. \quad (16)$$

From (9), by ignoring higher-order terms,  $e_k^+$  and  $e_k^-$  satisfy the following linearized equation:

$$e_k^+ = \Psi_k e_k^- - K_k v_k \quad (17)$$

where a filter transition matrix  $\Psi_k$  is defined as

$$\Psi_k = I - K_k H_k. \quad (18)$$

In general, EKF works well if the functions  $f$  and  $h$ , and the matrices  $F_k$ ,  $H_k$ ,  $Q_k$ , and  $R_k$  accurately approximate the actual system. However, it often suffers from model errors, and inaccurate models tend to result in large or biased estimation errors; in particular, process model uncertainties may cause filter divergence [17], [18].

One approach to coping with the model errors is to add fictitious noises to  $w_k$  and  $v_k$  and inflate  $Q_k$  and  $R_k$  appropriately. The inflated  $Q_k$  and  $R_k$  may cover uncertainties due to model errors and mitigate unexpectedly large or biased estimation errors. However, it would be difficult to find appropriate fictitious noises, especially for the systems where the number and quality of measurements vary with the environment. If fictitious noises are chosen in a naïve manner, the filter performance can be even worse [5], [6].

In this article, we consider adding fictitious noise to the process model in (3) based on the measurement matrix  $H_k$ . In Section II-B, when the process noise covariance is bumped up as  $Q_k + \delta Q_k$  by fictitious noises, we will analyze the variations of  $P_k^+$  and  $K_k$  due to  $\delta Q_k$ .

### B. Sensitivity Due to Fictitious Process Noise

In this section, we assume that filter computations at time step  $k-1$  are completed and  $P_{k-1}^+$  is given and that a fictitious noise is added to  $w_k$  at time step  $k$ . Then, in the EKF expressed in (7)–(14), (8) is replaced by the following equation:

$$P_k^-(\delta Q_k) = F_{k-1} P_{k-1}^+ F_{k-1}^T + Q_k + \delta Q_k \quad (19)$$

where  $\delta Q_k$  is a positive semidefinite matrix in  $\mathbb{R}^{n \times n}$  that corresponds to the fictitious noise.

The variations of  $P_k^+$  and  $K_k$  due to  $\delta Q_k$  are defined as

$$\Delta K_k \equiv K_k(\delta Q_k) - K_k(O) \quad (20)$$

$$\Delta P_k \equiv P_k^+(\delta Q_k) - P_k^+(O). \quad (21)$$

Note that  $P_k^-$ ,  $P_k^+$ , and  $K_k$  are expressed as the functions of  $\delta Q_k$ , that is,  $P_k^-(\delta Q_k)$ ,  $P_k^+(\delta Q_k)$ , and  $K_k(\delta Q_k)$ , in (19)–(21). When  $\delta Q_k$  is a zero matrix, they are denoted as  $P_k^-(O)$ ,  $P_k^+(O)$ , and  $K_k(O)$  that coincide with those in the EKF without fictitious noise.

For a given  $\delta Q_k$ ,  $\Delta K_k$  and  $\Delta P_k$  can be calculated from the following lemma.

*Lemma 1:*  $\Delta K_k$  and  $\Delta P_k$  satisfy the following equations:

$$\Delta K_k = \Delta P_k H_k^T R_k^{-1} \quad (22)$$

$$\begin{aligned} \Delta P_k &= [I - K_k(O)H_k]\delta Q_k \\ &\times \{[I - K_k(O)H_k]^{-T} + H_k^T R_k^{-1} H_k \delta Q_k\}^{-1}. \end{aligned} \quad (23)$$

*Proof:* From (14) and (21),

$$\begin{aligned} K_k(\delta Q_k) &= P_k^+(\delta Q_k) H_k^T R_k^{-1} \\ &= [P_k^+(O) + \Delta P_k] H_k^T R_k^{-1}. \end{aligned}$$

Substituting the above equation into (20), we have (22). From (10),

$$\begin{aligned} P_k^+(\delta Q_k) &= [I - K_k(\delta Q_k)H_k]P_k^-(\delta Q_k) \\ &= [I - (K_k(O) + \Delta K_k)H_k](P_k^-(O) + \delta Q_k). \end{aligned}$$

Substituting (22) into the above equation and noting that  $[I - K_k(O)H_k]^{-T} = I + H_k^T R_k^{-1} H_k P_k^-(O)$  from (10) and (12), we obtain (23).  $\square$

On the other hand, if  $\Delta P_k$  is given, the corresponding value of  $\delta Q_k$  can be obtained from the following lemma.

*Lemma 2:* Under the assumption that  $P_k^-(\delta Q_k)$  is positive definite,  $\delta Q_k$  corresponding to a given  $\Delta P_k$  is obtained as

$$\begin{aligned} \delta Q_k &= [I - (K_k(O) + \Delta K_k)H_k]^{-1} \\ &\times [\Delta P_k - \Delta K_k(H_k P_k^-(O) H_k^T + R_k) \Delta K_k^T] \\ &\times [I - (K_k(O) + \Delta K_k)H_k]^{-T} \end{aligned} \quad (24)$$

where  $\Delta K_k$  is calculated from (22).

*Proof:* From (11),  $\Delta P_k$  in (21) can be written as

$$\begin{aligned} \Delta P_k &= [I - (K_k(O) + \Delta K_k)H_k] \\ &\times [P_k^-(O) + \delta Q_k] \\ &\times [I - (K_k(O) + \Delta K_k)H_k]^T \\ &+ (K_k(O) + \Delta K_k)R_k(K_k(O) + \Delta K_k)^T \\ &- [I - K_k(O)H_k]P_k^-(O)[I - K_k(O)H_k]^T \\ &- K_k(O)R_k K_k^T(O) \end{aligned}$$

$$\begin{aligned} &= [I - (K_k(O) + \Delta K_k)H_k]\delta Q_k \\ &\times [I - (K_k(O) + \Delta K_k)H_k]^T \\ &+ \Delta K_k[H_k P_k^-(O) H_k^T + R_k] \Delta K_k^T \end{aligned} \quad (25)$$

where we used the following equation:

$$\begin{aligned} \Delta K_k R_k K_k^T(O) &= \Delta K_k R_k R_k^{-1} H_k P_k^+(O) \\ &= \Delta K_k H_k P_k^+(O) \\ &= \Delta K_k H_k P_k^-(O)(I - K_k(O)H_k)^T. \end{aligned}$$

By solving (25) for  $\delta Q_k$ , we have (24). Note that  $[I - (K_k(O) + \Delta K_k)H_k]^{-1}$  always exists because

$$\begin{aligned} &[I - (K_k(O) + \Delta K_k)H_k]^{-1} \\ &= [I - P_k^+(\delta Q_k) H_k^T R_k^{-1} H_k]^{-1} \\ &= [(P_k^+(\delta Q_k))^{-1} - H_k^T R_k^{-1} H_k]^{-1} (P_k^+(\delta Q_k))^{-1} \\ &= P_k^-(\delta Q_k) (P_k^+(\delta Q_k))^{-1} \\ &= I + P_k^-(\delta Q_k) H_k^T R_k^{-1} H_k \end{aligned}$$

where from (12) and  $P_k^-(\delta Q_k) > 0$ , we used

$$(P_k^+(\delta Q_k))^{-1} = (P_k^-(\delta Q_k))^{-1} + H_k^T R_k^{-1} H_k.$$

$\square$

It should be noted that, while the filter is working properly, we can expect that  $P_k^-(O) > 0$  and the assumption that  $P_k^-(\delta Q_k) > 0$  would hold. If  $P_k^-(O) > 0$ ,  $P_k^-(\delta Q_k)$  is positive definite from (19) for  $\delta Q_k \geq 0$ . In addition,  $\Delta P_k$  is a positive semidefinite matrix from (25) for  $\delta Q_k \geq 0$ .

### III. ADAPTIVE CHOICE OF PROCESS NOISE COVARIANCE

#### A. Minimization of Measurement Residuals

In the Kalman Filter, the Kalman gain  $K_k$  is derived so that the trace of the covariance matrix for  $e_k^+$ , that is,  $E\{\|e_k^+\|^2\}$  is minimized [17], where  $E\{a\}$  means the expected value of a random variable  $a$ . In this article, utilizing the parameter  $\delta Q_k$ , we minimize the expected value of measurement residual to build a filter that gives more credence to the recent measurement without using the measurement itself. The measurement residual  $m_k$  is represented as a function of  $\delta Q_k$  by the following equation:

$$\begin{aligned} m_k(\delta Q_k) &\equiv y_k - h(\hat{x}_k^+(\delta Q_k)) \approx H_k(x_k - \hat{x}_k^+(\delta Q_k)) + v_k \\ &= H_k e_k^+(\delta Q_k) + v_k. \end{aligned} \quad (26)$$

There are two reasons to focus on the measurement residual  $m_k(\delta Q_k)$ . First, many adaptive filtering approaches utilize the measurements to modify  $Q_k$  and  $R_k$ , because we can see the estimation accuracy only through the measurement residuals or innovations. Even though we use no measurement directly unlike conventional adaptive filters, the idea of modifying the filter based on the measurements would be reasonable. Second, only the component of  $e_k^+$  that corresponds to the measurement residual can be reduced by using  $\delta Q_k$  as shown in Appendix A.

Denoting  $I - K_k(O)H_k$  as  $\Psi_k(O)$ ,  $e_k^+(\delta Q_k)$  can be approximated as follows:

$$e_k^+(\delta Q_k) = x_k - \hat{x}_k^+(\delta Q_k)$$

$$\begin{aligned} &\approx [I - (K_k(O) + \Delta K_k)H_k]e_k^- - (K_k(O) + \Delta K_k)v_k \\ &= (\Psi_k(O) - \Delta P_k H_k^T R_k^{-1} H_k)e_k^- \\ &\quad - (K_k(O) + \Delta P_k H_k^T R_k^{-1})v_k. \end{aligned} \quad (27)$$

Substituting (27) into (26), the measurement residual  $m_k(\delta Q_k)$  can be rewritten as

$$\begin{aligned} m_k(\delta Q_k) &= H_k[(\Psi_k(O) - \Delta P_k H_k^T R_k^{-1} H_k)e_k^- \\ &\quad - (K_k(O) + \Delta P_k H_k^T R_k^{-1})v_k] + v_k. \end{aligned} \quad (28)$$

To formulate the problem of minimizing  $m_k(\delta Q_k)$ , we introduce the following function:

$$\begin{aligned} J_k(\Delta P_k) &= E\left\{\|m_k(\delta Q_k)\|_{R_k^{-1}}^2\right\} \\ &= E\left\{\left\|(\Psi_k(O) - \Delta P_k H_k^T R_k^{-1} H_k)e_k^-\right\|_{H_k^T R_k^{-1} H_k}^2\right\} \\ &\quad + E\left\{\left\|(I - H_k K_k(O) - H_k \Delta P_k H_k^T R_k^{-1})v_k\right\|_{R_k^{-1}}^2\right\}. \end{aligned} \quad (29)$$

It should be noted that the objective function  $J_k$  is defined as a function of  $\Delta P_k$ . Since Lemma 2 gives  $\delta Q_k$  corresponding to  $\Delta P_k$ , we can choose  $\Delta P_k$  as the decision variable instead of  $\delta Q_k$ . Moreover, we denote a norm of a vector  $b$  with a weighting matrix  $W$  as

$$\|b\|_W^2 = b^T W b.$$

Minimizing (29) gives

$$\Delta P_k^* = \operatorname{argmin}_{\Delta P_k} J_k(\Delta P_k). \quad (30)$$

Substituting  $\Delta P_k = \Delta P_k^*$  into (24), we have

$$\begin{aligned} \delta Q_k^* &= [I - (K_k(O) + \Delta K_k^*)H_k]^{-1} \\ &\quad \times [\Delta P_k^* - \Delta K_k^*(H_k P_k^-(O) H_k^T + R_k) \Delta K_k^{*T}] \\ &\quad \times [I - (K_k(O) + \Delta K_k^*)H_k]^{-T} \end{aligned} \quad (31)$$

where  $\Delta K_k^* = \Delta P_k^* H_k^T R_k^{-1}$  from (22).

### B. Restriction on Fictitious Noise

Although the minimization problem is formulated by (30) in Section III-A, it would be difficult to find the optimal solution  $\Delta P_k^*$  among all  $n \times n$  positive semidefinite matrices. In this article, we will find the solution of (30) by restricting  $\Delta P_k$  to a certain form.

To introduce the form of  $\Delta P_k$ , we make the following assumption in this section.

*Assumption 1:* For the measurement matrix  $H_k \in \mathbb{R}^{m \times n}$ ,  $\operatorname{rank}(H_k) = m \leq n$ , that is,  $(H_k H_k^T)^{-1}$  exists.

Under the assumption,  $H_k$  can be represented through singular value decomposition as follows:

$$H_k = G_k \Sigma_k S_k^T \quad (32)$$

where  $G_k \in \mathbb{R}^{m \times m}$  and  $S_k \in \mathbb{R}^{n \times n}$  are orthogonal matrices and  $\Sigma_k \in \mathbb{R}^{m \times n}$  is expressed as

$$\Sigma_k = (\tilde{\Sigma}_k \quad O_{m \times (n-m)}). \quad (33)$$

$\tilde{\Sigma}_k \in \mathbb{R}^{m \times m}$  is a diagonal matrix whose diagonal elements are nonzero singular values of  $H_k$ . Since  $H_k^T R_k^{-1} H_k$  is symmetric, it can be represented as

$$H_k^T R_k^{-1} H_k = S_k \begin{pmatrix} \Lambda_k & O_{m \times (n-m)} \\ O_{(n-m) \times m} & O_{(n-m) \times (n-m)} \end{pmatrix} S_k^T \quad (34)$$

where  $\Lambda_k \in \mathbb{R}^{m \times m}$  is a positive definite matrix whose eigenvalues are positive eigenvalues of  $H_k^T R_k^{-1} H_k$ .

Then, we restrict the decision variable  $\Delta P_k$  to the following form:

$$\Delta P_k = \alpha_k H_k^T R_k^{-1} H_k + \beta_k \mathcal{H}_k^\perp \quad (35)$$

where  $\alpha_k$  and  $\beta_k$  are nonnegative scalar parameters, and  $\mathcal{H}_k^\perp$  is defined using an arbitrary positive semidefinite matrix  $\Lambda_k^\perp \in \mathbb{R}^{(n-m) \times (n-m)}$  as

$$\mathcal{H}_k^\perp = S_k \begin{pmatrix} O_{m \times m} & O_{m \times (n-m)} \\ O_{(n-m) \times m} & \Lambda_k^\perp \end{pmatrix} S_k^T. \quad (36)$$

Note that the following equation is satisfied:

$$H_k \mathcal{H}_k^\perp = O_{m \times n}. \quad (37)$$

In the rest of this section, we will describe the choice of the parameter  $\beta_k$ , because  $\alpha_k$  will be obtained through minimization of  $J_k(\Delta P_k)$  in Section III-C. Substituting (35) into (29) and using (37), we obtain

$$\begin{aligned} J_k(\Delta P_k) &= E\left\{\left\|(\Psi_k(O) - \alpha_k(H_k^T R_k^{-1} H_k)^2)e_k^-\right\|_{H_k^T R_k^{-1} H_k}^2\right\} \\ &\quad + E\left\{\left\|(I - H_k K_k(O) - \alpha_k H_k H_k^T R_k^{-1} H_k H_k^T R_k^{-1})v_k\right\|_{R_k^{-1}}^2\right\}. \end{aligned} \quad (38)$$

From (38), the objective function  $J_k(\Delta P_k)$  is dependent only on  $\alpha_k$  by restricting  $\Delta P_k$  to the form of (35).<sup>1,2</sup>

Since  $J_k(\Delta P_k)$  is independent of  $\beta_k$ , we can choose any nonnegative values of  $\beta_k$  in the sense of minimizing  $J_k(\Delta P_k)$ . However, nonzero  $\beta_k$  often makes the estimation error covariance matrix  $P_k^+$  excessively large and causes severe degradation of filter performance especially at the time step when  $H_k$  changes significantly from the previous ones  $H_{k-i}$ , as described in Appendix B. Therefore, we choose  $\beta_k = 0$  in this article, and then,  $\Delta P_k$  becomes

$$\Delta P_k = \alpha_k H_k^T R_k^{-1} H_k. \quad (39)$$

<sup>1</sup>Even if  $\alpha_k H_k^T R_k^{-1} H_k$  is replaced by  $\alpha_k H_k^T C_k H_k$  with an arbitrary positive semidefinite matrix  $C_k$  in (35),  $J_k(\Delta P_k)$  is dependent only on  $\alpha_k$ . That is,  $C_k$  can also be a parameter in the proposed method. Although we choose  $C_k$  as  $R_k^{-1}$  in this article, a more appropriate choice of  $C_k$  for better performance remains a topic for future work. At least, for the numerical example in Section IV, the choice of  $C_k = R_k^{-1}$  achieved better performance, compared to the choice of  $C_k = I$  or  $C_k = R_k^{-1} H_k^T H_k R_k^{-1}$ .

<sup>2</sup>If not restricted to the form of (35),  $\Delta P_k$  can be represented as  $\Delta P_k = \alpha_k H_k^T C_k H_k + \beta_k \mathcal{H}_k^\perp + \gamma_k \mathcal{H}_k^\perp$ , where  $\gamma_k$  is a scalar and  $\mathcal{H}_k^\perp$  is defined as  $\mathcal{H}_k^\perp = S_k \begin{pmatrix} O_{m \times m} & \Lambda_k^\perp \\ \Lambda_k^\perp & O_{(n-m) \times (n-m)} \end{pmatrix} S_k^T$  with  $\Lambda_k^\perp \in \mathbb{R}^{m \times (n-m)}$ . Even then, since  $H_k \mathcal{H}_k^\perp H_k^T = O_{m \times m}$ , a similar equation to (38) is satisfied, and the cost function  $J(\Delta P_k)$  is independent of  $\gamma_k$  as well as  $\beta_k$ . However, to guarantee that  $\Delta P_k$  is a positive semidefinite matrix, we have to choose  $\beta_k \mathcal{H}_k^\perp$  and  $\gamma_k \mathcal{H}_k^\perp$  so that they satisfy a certain inequality. In addition, Appendix B holds only when  $\gamma_k = 0$ . In this article, we choose  $\gamma_k$  as zero for simplicity.

### C. H-Adaptive Filter

In this section, we find the solution  $\Delta P_k^*$  of the minimization problem (30) under the condition that  $\Delta P_k$  is restricted to the form of (39). Since the decision variable is reduced to only  $\alpha_k$ , we can obtain  $\Delta P_k^*$  analytically.

To derive the analytical solution that does not need the measurements  $y_k$  themselves, we make the following assumption:

*Assumption 2:*  $E\{(e_k^-)(e_k^-)^T\}$  can be approximated as  $E\{(e_k^-)(e_k^-)^T\} = P_k^-$ .

For brevity of notation, we denote  $H_k^T R_k^{-1} H_k$  as  $\mathcal{O}_k$  in this section.

Noticing that we can suppose that  $\mathcal{O}_k$  is a nonzero and positive semidefinite matrix,  $\Delta P_k^*$  is given by the following lemma.

*Lemma 3:* Under Assumption 2, the solution to the minimization problem (30) is derived for  $\Delta P_k$  in the form of (39) as follows:

$$\Delta P_k^* = \alpha_k^* \mathcal{O}_k \quad (40)$$

$$\alpha_k^* = \frac{\text{tr} [\mathcal{O}_k^2]}{\text{tr} [\mathcal{O}_k^5 P_k^- + \mathcal{O}_k^4]}. \quad (41)$$

*Proof:* Since  $J(\Delta P_k)$  is a quadratic function of  $\alpha_k$ , we can solve the problem by finding  $\alpha_k^*$  that satisfies

$$\left. \frac{\partial J(\Delta P_k)}{\partial \alpha_k} \right|_{\alpha_k=\alpha_k^*} = 0. \quad (42)$$

The left-hand side of (42) can be calculated as

$$\begin{aligned} & \frac{1}{2} \frac{\partial J(\Delta P_k)}{\partial \alpha_k} \\ &= E\{-e_k^{-T} \mathcal{O}_k^3 \Psi_k(O) e_k^- + \alpha_k e_k^{-T} \mathcal{O}_k^5 e_k^- \\ &\quad - v_k^T R_k^{-1} H_k \mathcal{O}_k H_k^T R_k^{-1} (I - H_k K_k(O)) v_k \\ &\quad + \alpha_k v_k^T R_k^{-1} H_k \mathcal{O}_k^3 H_k^T R_k^{-1} v_k\} \\ &= \text{tr} [\alpha_k \mathcal{O}_k^5 P_k^-] - \text{tr} [\mathcal{O}_k^3 P_k^- \Psi_k^T(O)] \\ &\quad + \text{tr} [\alpha_k \mathcal{O}_k^4] - \text{tr} [H_k \mathcal{O}_k H_k^T (I - H_k K_k(O))^T R_k^{-1}] \\ &= \alpha_k \text{tr} [\mathcal{O}_k^5 P_k^- + \mathcal{O}_k^4] - \text{tr} [\mathcal{O}_k^2] \end{aligned} \quad (43)$$

where we used (14) and the following equations:

$$\begin{aligned} & \text{tr} [H_k \mathcal{O}_k H_k^T (I - H_k K_k(O))^T R_k^{-1}] \\ &= \text{tr} [H_k \mathcal{O}_k H_k^T R_k^{-1} - H_k \mathcal{O}_k H_k^T K_k^T(O) H_k^T R_k^{-1}] \\ &= \text{tr} [\mathcal{O}_k^2] - \text{tr} [K_k(O) H_k \mathcal{O}_k^2] \\ & \text{tr} [\mathcal{O}_k^3 P_k^- \Psi_k^T(O)] = \text{tr} [\mathcal{O}_k^2 H_k^T R_k^{-1} H_k P_k^+(O)] \\ &= \text{tr} [K_k(O) H_k \mathcal{O}_k^2]. \end{aligned}$$

From (42) and (43), we obtain (41).

It should be noted that, from (41),  $\alpha_k^*$  satisfies  $\alpha_k^* > 0$ .

From Lemma 1–3, the filter proposed in this article is summarized as follows.

Time update:

$$\begin{aligned} \hat{x}_k^- &= f(\hat{x}_{k-1}^+) \\ P_k^-(\delta Q_k^*) &= F_{k-1} P_{k-1}^+ F_{k-1}^T + Q_{k-1} + \delta Q_k^*. \end{aligned} \quad (44)$$

Measurement update:

$$\hat{x}_k^+(\delta Q_k^*) = \hat{x}_k^- + K_k(\delta Q_k^*)[y_k - h(\hat{x}_k^-)] \quad (45)$$

$$\begin{aligned} P_k^+(\delta Q_k^*) &= [I - K_k(\delta Q_k^*) H_k] P_k^-(\delta Q_k^*) \\ &= P_k^+(O) + \Delta P_k^* \end{aligned} \quad (46)$$

$$\begin{aligned} K_k(\delta Q_k^*) &= P_k^-(\delta Q_k^*) H_k^T [H_k P_k^-(\delta Q_k^*) H_k^T + R_k]^{-1} \\ &= K_k(O) + \Delta K_k^* \end{aligned} \quad (47)$$

where

$$\mathcal{O}_k = H_k^T R_k^{-1} H_k$$

$$\alpha_k^* = \frac{\text{tr} [\mathcal{O}_k^2]}{\text{tr} [\mathcal{O}_k^5 P_k^- + \mathcal{O}_k^4]}$$

$$\Delta P_k^* = \alpha_k^* \mathcal{O}_k$$

$$\Delta K_k^* = \Delta P_k^* H_k^T R_k^{-1}$$

$$\begin{aligned} \delta Q_k^* &= [I - (K_k(O) + \Delta K_k^*) H_k]^{-1} \\ &\quad \times [\Delta P_k^* - \Delta K_k^* (H_k P_k^-(O) H_k^T + R_k) \Delta K_k^{*T}] \\ &\quad \times [I - (K_k(O) + \Delta K_k^*) H_k]^{-T}. \end{aligned}$$

In the above filter, fictitious noise  $\delta Q_k^*$  is chosen at each time step depending on the measurement matrix  $H_k$ , not on the measurement itself. Therefore, we call the filter with the proposed choice of fictitious noise  $H$ -adaptive filter.

The  $H$ -adaptive filter inflates the estimation error covariance matrix  $P_k^+$  in the row space of  $H_k$ . Thus, the  $H$ -adaptive filter forgets information to some extent in the row space of  $H_k$  compared to the standard Kalman filter. In this sense, it can be regarded as one FMF. However, the conventional FMF forgets information uniformly in every direction [4], while the  $H$ -adaptive filter forgets only in the row space of  $H_k$ . Since new information can be obtained in the row space of  $H_k$  at time step  $k$ , forgetting some prior information in the row space would not degrade the estimation accuracy. On the other hand, forgetting prior information perpendicular to the row space of  $H_k$  excessively would lead to the degradation of estimation accuracy, because no information in that direction is provided from the measurement.

To construct the  $H$ -adaptive filter, we made Assumption 2. Since the assumption is only used to calculate  $\alpha_k^*$  in (41), the value of  $\alpha_k^*$  may be far away from its optimal value if the assumption is violated. If  $\alpha_k^*$  is much smaller than the optimal value due to the violation, the estimates with that smaller  $\alpha_k^*$  will approach the estimates for the EKF. This is because the EKF is equivalent to the filter with  $\alpha_k^* = 0$ , that is,  $\delta Q_k^* = O$ . On the other hand, if  $\alpha_k^*$  is larger than the optimal value, the performance of the filter may degrade. The sensitivity of the estimates to the violation of Assumption 2 should be examined carefully in the future, although we checked that the estimation accuracy does not change significantly for some deviations in the value of  $\alpha_k^*$  for the numerical example in Section IV. In addition, if  $\alpha_k^*$  is excessively larger,  $\delta Q_k^*$  might not be positive semidefinite, as described below.

Lemma 2 does not guarantee that  $\delta Q_k^*$  corresponding to  $\Delta P_k^*$  is a positive semidefinite matrix, although  $\delta Q_k^*$  was always positive semidefinite in the numerical and experimental examples shown in Sections IV and V. If  $\delta Q_k^*$  is not positive semidefinite in the above filter, we can replace at that time step (40) with  $\Delta P_k^* = s_k \alpha_k^* \mathcal{O}_k$  to get a positive semidefinite  $\delta Q_k^*$  by using  $s_k \in (0, 1)$ .

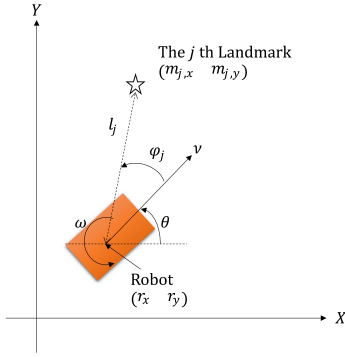


Fig. 1. Localization of a mobile robot.

#### IV. NUMERICAL DEMONSTRATION

##### A. Localization of Mobile Robot

In this section, we demonstrate the effectiveness of the  $H$ -adaptive filter through numerical simulations for localization of a mobile robot [3]. We consider a mobile robot that moves on the  $XY$  plane where there are several landmarks, as in Fig. 1. The position and heading angle of the robot are denoted as  $r = (r_x, r_y)^T$  [m] and  $\theta$  [rad], respectively. The position of the  $j$ th landmark is represented as  $m_j = (m_{j,x}, m_{j,y})^T$  [m], and assumed to be known. It is also supposed that a LiDAR is installed in the robot along its heading to measure distances and angles from the robot to visible landmarks. Measurements from the  $j$ th landmark are expressed as  $y_j = (l_j, \varphi_j)^T$ , where  $l_j$  [m] is the distance and  $\varphi_j$  [rad] is the angle.

The state and velocity input vectors for the robot are defined as  $x = (r_x, r_y, \theta)^T$  and  $u = (v, \omega)^T$ , where  $v$  [m/s] is the translational velocity and  $\omega$  [rad/s] is the angular velocity. The state and measurement equations are as follows:

$$\begin{aligned} x_k &= f(x_{k-1}, u_k) \\ &= x_{k-1} + \begin{pmatrix} v_k \omega_k^{-1} [\sin(\theta_{k-1} + \omega_k \Delta t) - \sin \theta_{k-1}] \\ v_k \omega_k^{-1} [-\cos(\theta_{k-1} + \omega_k \Delta t) + \cos \theta_{k-1}] \\ \omega_k \Delta t \end{pmatrix} \end{aligned} \quad (48)$$

$$\begin{aligned} y_{j,k} &= h_j(x_k) + v_{j,k} \\ &= \left( \sqrt{(m_{j,x} - r_{k,x})^2 + (m_{j,y} - r_{k,y})^2} \right. \\ &\quad \left. \arctan 2((m_{j,y} - r_{k,y}), (m_{j,x} - r_{k,x})) - \theta \right) \\ &\quad + v_{j,k} \end{aligned} \quad (49)$$

where  $v_{j,k}$  is a Gaussian measurement noise, that is,  $v_{j,k} \sim N(0, R_{j,k})$ . Note that, if  $\omega_k = 0$ , (48) becomes  $x_k = x_{k-1} + (v_k \Delta t \cos(\theta_{k-1}), v_k \Delta t \sin(\theta_{k-1}), 0)^T$ .

The uncertainties in the process model (48) are introduced by adding a disturbance  $w_k$  to the velocity vector  $u_k$  as

$$u'_k = u_k + w_k. \quad (50)$$

The disturbance  $w_k$  was set based on [3] in the simulations below, assuming that it consists of two components: bias due to, for example, the load imbalance of a robot and random noise due to, for example, pebbles on the robot's path.

Then, (48) is replaced with

$$x_k = f(x_{k-1}, u'_k). \quad (51)$$

##### B. Simulation Results

We performed numerical simulations where the robot moves at  $u_k = (0.2, 0.0)^T$  ( $k \geq 1$ ) from  $x_0 = (-2.0, 0, 0)^T$  on the  $XY$  plane. Three landmarks whose positions are  $(m_{1,x}, m_{1,y}) = (4.5, 0)$ ,  $(m_{2,x}, m_{2,y}) = (4.5, 2.0)$ , and  $(m_{3,x}, m_{3,y}) = (4.5, -2.0)$  exist on the plane. In [3], the  $j$ th landmark is assumed to be visible when it satisfies the following conditions:  $|\bar{l}_j| < \varepsilon_l \wedge |\bar{\varphi}_j| < \varepsilon_\varphi$  for  $j = 1$  and  $|\bar{l}_j| < \varepsilon_l \wedge |\bar{\varphi}_j| < \varepsilon_\varphi \wedge z_{j,k} > \varepsilon$  for  $j = 2, 3$ , where  $\bar{l}_j$  and  $\bar{\varphi}_j$  are the true distance and angle of the  $j$ th landmark, respectively, and  $z_{j,k}$  is a uniformly distributed random variable on  $[0, 1]$ . The parameters  $\varepsilon_l$ ,  $\varepsilon_\varphi$ , and  $\varepsilon$  were chosen as 6.0 [m],  $\pi/3$  [rad], and 0.99 respectively. These conditions mean that measurements  $y_{2,k}$  and  $y_{3,k}$  can rarely be obtained due to large  $\varepsilon$ , that is, the observability is degenerate at almost all time steps. The numerical simulations were done 25 times with different noise sequences  $\{w_k\}$  and  $\{v_k\}$  for the filters in the three settings mentioned below, where the time step  $k$  ranged from 0 to 250 with  $\Delta t = 0.1$  [s].

The following three settings were used to construct the EKF for localization of the robot.

*Setting (1):* The filter is a conventional EKF with

$$\delta Q_k = O. \quad (52)$$

*Setting (2):* The filter corresponds to FMF [4], [7] by choosing  $\delta Q_k$  as

$$\delta Q_k = c F_{k-1} P_{k-1}^+ F_{k-1} \quad (53)$$

where  $c = 0.04$ .

*Setting (3):* The filter is  $H$ -adaptive filter with

$$\delta Q_k = \delta Q_k^* \quad (54)$$

where  $\delta Q_k^*$  is given by (31).

In Setting (2),  $c$  was set to be 0.04, because the estimation accuracy with  $c = 0.04$  was the highest among those with  $c = \{0.01, 0.02, \dots, 0.07\}$ . In all the settings, the nominal  $Q_k$  is computed at each time step assuming the covariances of the noises in  $v_k$  and  $\omega_k$  to be 0.0025 and 0.0027, respectively, and the nominal  $R_{j,k}$  is given as  $\text{diag}(0.01, 0.001)$ .

To illustrate the accuracy difference among the three settings, the behaviors of the true robot and the estimated state on the  $XY$  plane for one set of noise sequences  $\{w_k\}$  and  $\{v_k\}$  are shown in Fig. 2 as an example. In the figure, the true position and estimated position of the robot are drawn by the black and blue lines, respectively. The estimation error covariance  $P_k^+$  calculated by the filter is also drawn in blue every 50 steps as a  $3\sigma$  ellipse [19]. The behaviors in each setting will be described below.

In Setting (1), the true position of the robot is outside the ellipse at the final time step in Fig. 2(a). We can see that the estimation error covariance matrix becomes very small, and the filter divergence is caused. It would be because the nominal  $Q_k$  is too small to cover the model error. Moreover,

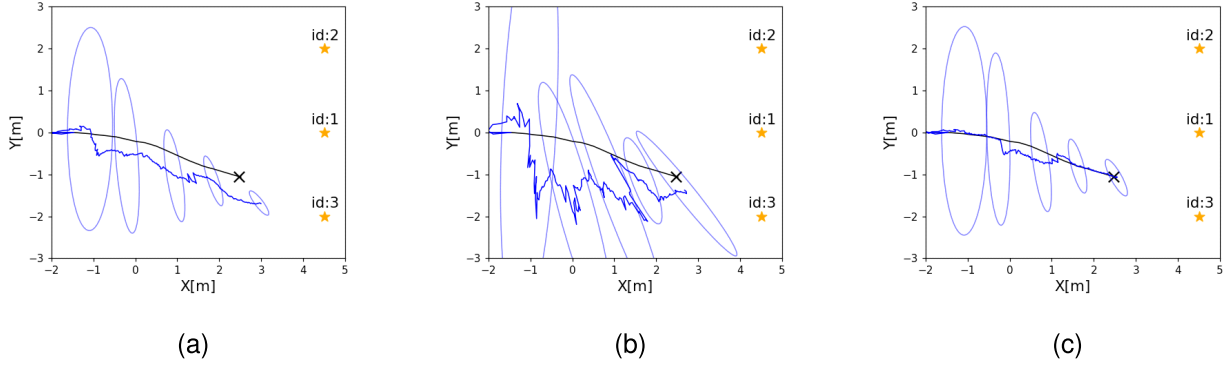


Fig. 2. Example of numerical results for localization of a robot by three filters. Black and blue lines are the true and estimated positions of the robot, respectively, and blue ellipses represent  $3\sigma$  error ellipses. (a) Setting (1): EKF. (b) Setting (2): FMF. (c) Setting (3):  $H$ -adaptive filter.

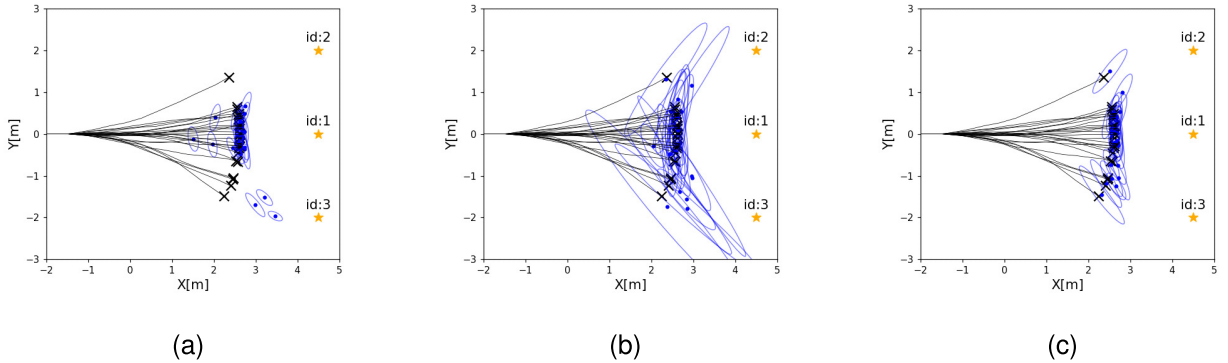


Fig. 3. Numerical results for all noise sequences. Black  $\times$  marks and lines are the true positions of the robot at the final step and the paths of the robot. Blue dots and ellipses represent estimated positions and  $3\sigma$  error ellipses at the final step, respectively. (a) Setting (1): EKF. (b) Setting (2): FMF. (c) Setting (3):  $H$ -adaptive filter.

the ratio of the major and minor axes of the final ellipse is 4.11.

In Setting (2), the true positions of the robot are inside the ellipses even at the final time step in Fig. 2(b), but all the ellipses are too large. The unnecessarily inflated ellipses cause very large estimation errors (see also Appendix B), although they avoid the filter divergence. Moreover, the ratio of the major and minor axes of the last ellipse is 10.2 in this setting. The ellipses are more inflated in the direction perpendicular to the line of sight of the first landmark as shown in Fig. 2(b), which results in the larger ratio compared to the one in Setting (1).

In Setting (3), the true positions are inside the ellipses at all the time steps, and the size of the ellipses looks to be kept reasonable. As a result, the  $H$ -adaptive filter achieves the highest estimation accuracy. The ratio of the major and minor axes is 4.09, which is close to the one in Setting (1). It indicates that the  $H$ -adaptive filter avoided excessive inflation of  $P_k^+$  along the direction perpendicular to the row space of  $H_k$  by choosing  $\beta_k = 0$ .

We finally show estimation results for all 25 noise sequences in Fig. 3 to examine variations due to noise sequences. The true and estimated positions of the robot at the final step  $k = 250$  are represented as black  $\times$  marks and blue dots, respectively. For Setting (1), only ten of the 25 true positions fall within the  $3\sigma$  error ellipses depicted in blue. For Setting (2), although all the 25 true positions are within the  $3\sigma$  error

TABLE I  
RMSEs IN STATE ESTIMATION AT THE FINAL TIME STEP

	$r_x$ [m]	$r_y$ [m]	$\theta$ [rad]
(1) Extended Kalman filter	0.32	0.55	0.29
(2) Fading memory filter	0.21	0.43	0.25
(3) $H$ -adaptive filter	0.10	0.17	0.12

ellipses, the ellipses and the estimation errors are quite large. Compared to the two settings, for Setting (3), the ellipses are properly inflated by the proposed filter and contain all the 25 true positions inside with small estimation errors. Table I summarizes the root mean squared error (RMSE) for 25 estimated states at the final time step  $k = 250$  for each setting. The highest accuracy was achieved using Setting (3), that is, the  $H$ -adaptive filter.

## V. APPLICATION

### A. GNSS/INS Positioning

This section presents a practical application of the  $H$ -adaptive filter to a vehicle positioning with GNSS and INS (Fig. 4). Since GNSS and INS are complementary in terms of error characteristics, their integration is commonly employed to improve positioning accuracy for automobiles. The integration is accomplished in a tightly coupled manner by the EKF as shown in Fig. 5.

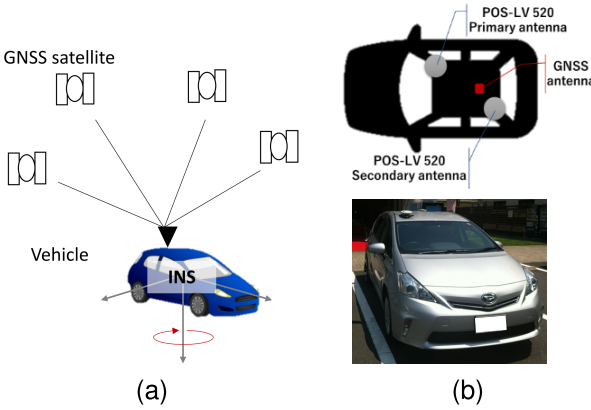


Fig. 4. Positioning system with GNSS/INS for a test vehicle. (a) Vehicle positioning with GNSS/INS. (b) Test vehicle.

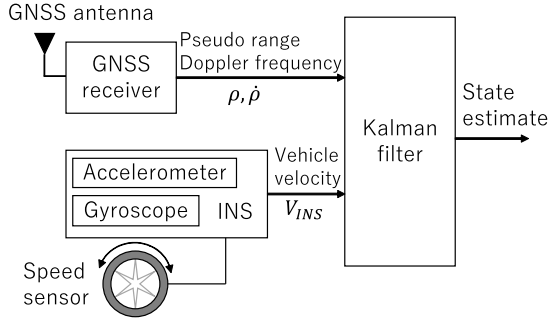


Fig. 5. Block diagram of a tightly coupled integration of GNSS and INS.

The state and measurement vectors are given as

$$x = (r^T, \delta t, \dot{r}^T, \delta \dot{t}, b^T)^T \quad (55)$$

$$y = (\rho^T, \dot{\rho}^T, v_{INS}^T)^T \quad (56)$$

where  $r$  [m] and  $\dot{r}$  [m/s] are position and velocity vectors in  $\mathbb{R}^3$ , respectively. They are represented in the Earth-Centered-Earth-Fixed (ECEF) coordinates that are commonly used in the GNSS applications [20]. The clock bias and drift of a GNSS receiver are denoted as  $\delta t$  [m] and  $\delta \dot{t}$  [m/s] in  $\mathbb{R}$ , respectively. When multiple ( $l + 1$ ) GNSS constellations such as GPS and Galileo are used for positioning, intersystem biases (ISBs), defined as the difference between the GPS's system clock and other GNSS systems' clock, are included as an  $l$ -dimensional vector  $b$  [m] in  $x$ . In the measurement vector  $y$ , pseudo-ranges and Doppler frequencies obtained from the signals of  $m$  satellites are denoted as  $\rho$  [m] and  $\dot{\rho}$  [m/s] in  $\mathbb{R}^m$ , respectively. The velocity vector provided from INS is represented as  $v_{INS} \in \mathbb{R}^3$ . For further details on GNSS/INS positioning, see, for example, [20], [21], [22].

The state and measurement equations for this system are

$$\begin{aligned} x_{k+1} &= f(x_k) + w_k \\ &= Fx_k + w_k \end{aligned} \quad (57)$$

$$y_k = h(x_k) + v_k \quad (58)$$

where denoting the  $i$ th element of  $h(x_k)$  as  $h_i(x_k)$ ,

$$h_i(x_k) = \begin{cases} \|r_k - r_k^i\| + \delta t_k + b_k(i), & 1 \leq i \leq m \\ e_{i,k}^T(\dot{r}_k - \dot{r}_k^i) + \delta \dot{t}_k, & m + 1 \leq i \leq 2m \end{cases} \quad (59)$$

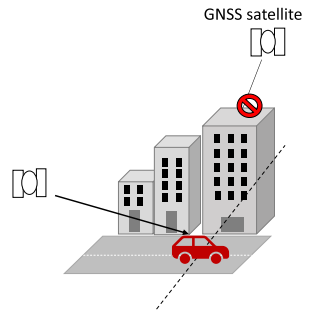


Fig. 6. Biased distribution of visible satellites in urban areas.

$$(h_{2m+1}(x_k), h_{2m+2}(x_k), h_{2m+3}(x_k))^T = \dot{r}_k \quad (60)$$

$$e_{i,k} = \frac{r_k - r_k^i}{\|r_k - r_k^i\|} \quad (61)$$

$$F = \begin{pmatrix} I_{4 \times 4} & \Delta t I_{4 \times 4} & O_{4 \times l} \\ O_{4 \times 4} & I_{4 \times 4} & O_{4 \times l} \\ O_{l \times 4} & O_{l \times 4} & I_{l \times l} \end{pmatrix}.$$

In (59),  $r_k^i$  denotes the position vector of satellite  $i$ , and  $b_k(i)$  is the ISB of the constellation that satellite  $i$  belongs to.

To construct the EKF, nominal noises  $Q_k$  and  $R_k$  are set based on [5], [20], [23], [24], and [6] as follows:

$$Q_k = \begin{pmatrix} Q_1 & \tilde{Q} & O_{4 \times l} \\ \tilde{Q}^T & Q_2 & O_{4 \times l} \\ O_{l \times 4} & O_{l \times 4} & 0.01 I_{l \times l} \end{pmatrix}, \quad \tilde{Q} = \begin{pmatrix} O_{3 \times 3} & O_{3 \times 1} \\ O_{1 \times 3} & 0.005 \end{pmatrix} \quad (62)$$

$$Q_1 = \begin{pmatrix} \text{diag}(0.16, 0.003\|v_{INS}\|^2, 10^{-5}) & O_{3 \times 1} \\ O_{1 \times 3} & 0.013 \end{pmatrix}$$

$$Q_2 = \begin{pmatrix} \text{diag}(0.64, 10^{-5}, 10^{-5}) & O_{3 \times 1} \\ O_{1 \times 3} & 0.01 \end{pmatrix}$$

$$R_k = \text{diag}(\sigma_1^2, \dots, \sigma_m^2, \dot{\sigma}_1^2, \dots, \dot{\sigma}_m^2, c_1, c_2, c_3) \quad (63)$$

where denoting the SNR of the signal from the  $i$ th satellite as  $s_i$  ( $i = 1, \dots, m$ ),  $\sigma_i = 0.64 + 784e^{-0.142s_i}$ ,  $\dot{\sigma}_i = 0.0125 + 6767e^{-0.267s_i}$ , and  $c_1 = c_2 = c_3 = 0.16$ .

However, note that the process model of the GNSS/INS integration mainly depends on INS accuracy. The INS accuracy often decreases due to unexpected sensor errors, which would make the process model inaccurate. Consequently, the above nominal  $Q_k$  may be relatively small.

In addition, it is also known that estimation accuracy in the lateral and vertical directions of a vehicle tends to degrade in urban areas [5], [6]. As shown in Fig. 6, satellite signals from the lateral direction of a vehicle are often blocked by obstacles such as tall buildings. The information from the satellite signals is nearly degenerate due to a biased distribution of visible satellites.

### B. Experimental Results

By using the test vehicle shown in Fig. 4, we collected the measurement data and performed the state estimation by the filters in the same three settings as in Section IV-B. Setting (1) for conventional EKF, Setting (2) for FMF, and Setting (3) for  $H$ -adaptive filter. Note that, in Setting (2), the parameter  $c$



Fig. 7. Route of the positioning experiment by a test vehicle in Nishinomiya city, Japan. It is shown by green dots obtained from the reference system (Applanix POS-LV 520).

was set to 0.03 in this experiment because the most accurate results were obtained when  $c = 0.03$ .

The measurements  $y$  were obtained by a vehicle positioning system (FURUNO GN-87, Bosch SMI130, and vehicle speed pulse sensor) installed in the test vehicle. A reference system (Applanix POS-LV 520) was also installed to provide highly accurate positions. We can calculate the positioning errors of the three filters by using the positions from the reference system as true positions.

The test vehicle made eight laps of the route shown in Fig. 7, running for 4330 s. The visibility of satellites from the vehicle varies significantly on the route. At A point, the vehicle is surrounded by a lot of objects located in its lateral direction. At B point, there is no object blocking the signals from the satellites to the vehicle.

We show the visibility of satellites on the route by introducing the well-known indicator called position dilution of precision (PDOP) [20]. PDOP at the time step  $k$  is defined as

$$\text{PDOP}(k) = \sqrt{\sum_{p=1}^3 [\tilde{H}_k^T \tilde{H}_k]_p^{-1}}$$

where  $[A]_p$  means the  $p$ th diagonal element of a matrix  $A$ , and, denoting the estimated value of  $e_{i,k}$  as  $\hat{e}_{i,k}$ ,

$$\tilde{H}_k = \begin{pmatrix} \hat{e}_{1,k} & \cdots & \hat{e}_{m,k} \\ 1 & \cdots & 1 \end{pmatrix}^T.$$

When PDOP is larger, the visibility of satellites is lower, and the positioning accuracy tends to degrade. The average value

TABLE II  
RMSEs AND MEAN ERRORS FOR POSITIONING ON THE ENTIRE ROUTE

	$x$ [m]	$y$ [m]	$z$ [m]	$\ e\ $ [m]
(1) Extended Kalman filter	2.0	2.2	4.4	2.9
(2) Fading memory filter	1.9	2.0	3.7	1.9
(3) $H$ -adaptive filter	1.9	1.8	3.1	1.5

TABLE III  
RMSEs AND MEAN ERRORS FOR POSITIONING AROUND A POINT

	$x$ [m]	$y$ [m]	$z$ [m]	$\ e\ $ [m]
(1) Extended Kalman filter	2.2	3.3	6.3	6.4
(2) Fading memory filter	2.2	3.1	3.9	4.3
(3) $H$ -adaptive filter	1.9	2.4	3.1	3.1

TABLE IV  
RMSEs AND MEAN ERRORS FOR POSITIONING AROUND B POINT

	$x$ [m]	$y$ [m]	$z$ [m]	$\ e\ $ [m]
(1) Extended Kalman filter	1.1	0.9	3.7	3.2
(2) Fading memory filter	1.1	0.9	1.7	1.0
(3) $H$ -adaptive filter	1.1	0.9	1.6	1.0

of PDOP for all the time steps of 4330 [sec] was 2.8, and the maximum and minimum values in the experiment were 15.8 and 1.8. At A point, PDOP was about 4.3, that is, the visibility was lower than at other points. At B point, PDOP was about 2.1, and the visibility was higher.

The positioning accuracies on the entire route in the three settings were computed as RMSEs in the body coordinate frame and are summarized in Table II, where  $x$ ,  $y$ , and  $z$  are RMSEs in the longitudinal (forward), lateral, and vertical directions of the vehicle, respectively. We can see that the accuracy in Setting (3) is the highest in every direction among them. In addition to the RMSEs, the mean error in each direction during the entire route was calculated to examine the bias error of the estimated position vector. The norms of the mean error vectors for the three settings are shown as  $\|e\|$  in Table II, indicating that the  $H$ -adaptive filter can reduce the mean error as well as the RMSEs. Although the measurement matrix  $H_k$  varies largely according to the visibility of satellites on the route, the  $H$ -adaptive filter provides highly accurate estimation by choosing the fictitious noise  $\delta Q_k$  appropriately.

To examine the positioning accuracy near A and B points, we computed the RMSEs and mean errors using the data from the time steps when the vehicle was in the neighborhood of each point. Tables III and IV show the results for A and B points, respectively, where the RMSEs and mean errors were calculated from 80 data points created by collecting ten time step data points around A or B point in each lap. The regions where the data was collected around A and B points are surrounded by red dashed curves in Fig. 7. In Table III for A point, the accuracies in all the settings degrade due to the lower visibility of satellites. However, the degradation is the smallest in Setting (3), and the  $H$ -adaptive filter achieves quite better accuracy compared to the other two filters. In Table IV for B point, the accuracies in all the settings become better because of the higher visibility of satellites. Even when sufficient information is obtained

from the measurements, the  $H$ -adaptive filter works well while achieving the same level of accuracy as the FMF.

## VI. CONCLUSION

This article proposed a novel method of choosing the process noise in the EKF based on the measurement matrix. When the inflation of the posterior estimation error covariance matrix due to a fictitious process noise is represented by two components, one based on the row space of the measurement matrix and the other perpendicular to that space, the latter does not affect the expected values of squared measurement residuals at each time step. Therefore, it was chosen as zero to avoid an unnecessary inflation of estimation error covariance for higher estimation accuracy. Then, the size of the former was determined by minimizing the expected values of squared measurement residuals. The method was applied to the EKF for vehicle positioning with GNSS/INS, and its effectiveness was demonstrated through actual driving tests, where the measurement matrix varied significantly during driving depending on the visibility of satellites.

## APPENDIX A

### REASON FOR MINIMIZING MEASUREMENT RESIDUAL

Under Assumption 1, we can divide  $e_k^*$  into  $e_{k,a}^*$  and  $e_{k,b}^*$  as follows:

$$\begin{aligned} e_k^* &= e_{k,a}^* + e_{k,b}^* \\ e_{k,a}^* &= P_{H_k} e_k^*, \quad e_{k,b}^* = (I - P_{H_k}) e_k^* \end{aligned} \quad (64)$$

where  $*$  means  $+$  or  $-$ , and  $P_{H_k}$  is a following projection matrix:

$$P_{H_k} = H_k^T (H_k H_k^T)^{-1} H_k. \quad (65)$$

Then, using  $\Psi_k(O) = I - K_k(O) H_k$ ,  $e_k^*(\delta Q_k)$  can be approximated as follows:

$$\begin{aligned} e_k^+(\delta Q_k) &\approx [I - (K_k(O) + \Delta K_k) H_k] e_k^- - (K_k(O) + \Delta K_k) v_k \\ &= (\Psi_k(O) - \Delta P_k H_k^T R_k^{-1} H_k) e_{k,a}^- + e_{k,b}^- \\ &\quad - (K_k(O) + \Delta P_k H_k^T R_k^{-1}) v_k. \end{aligned} \quad (66)$$

Furthermore, we obtain

$$\begin{aligned} e_{k,a}^+(\delta Q_k) &= P_{H_k} (\Psi_k(O) - \Delta P_k H_k^T R_k^{-1} H_k) e_{k,a}^- \\ &\quad - P_{H_k} (K_k(O) + \Delta P_k H_k^T R_k^{-1}) v_k \end{aligned} \quad (67)$$

$$\begin{aligned} e_{k,b}^+(\delta Q_k) &= (I - P_{H_k}) (\Psi_k(O) - \Delta P_k H_k^T R_k^{-1} H_k) e_{k,a}^- \\ &\quad + e_{k,b}^- - (I - P_{H_k}) (K_k(O) + \Delta P_k H_k^T R_k^{-1}) v_k. \end{aligned} \quad (68)$$

When  $\Delta P_k$  is chosen from (35) as  $\Delta P_k = \alpha_k H_k^T R_k^{-1} H_k + \beta_k \mathcal{H}_k^\perp$  in this article, (68) can be rewritten as

$$\begin{aligned} e_{k,b}^+(\delta Q_k) &= (I - P_{H_k}) \Psi_k(O) e_{k,a}^- + e_{k,b}^- \\ &\quad - (I - P_{H_k}) K_k(O) v_k = e_{k,b}^+(O) \end{aligned} \quad (69)$$

which means that  $e_{k,b}^+(\delta Q_k)$  does not depend on  $\delta Q_k$  or  $\Delta P_k$ . Therefore, the norm of  $e_k^+(\delta Q_k)$  can be represented as

$$\|e_k^+(\delta Q_k)\|^2 = \|e_{k,a}^+(\delta Q_k)\|^2 + \|e_{k,b}^+(\delta Q_k)\|^2$$

$$= \|e_{k,a}^+(\delta Q_k)\|^2 + \|e_{k,b}^+(O)\|^2. \quad (70)$$

Since  $\|e_{k,a}^+(\delta Q_k)\|^2 = \|H_k e_k^+(\delta Q_k)\|_{(H_k H_k^T)^{-1}}^2 \approx \|m_k(\delta Q_k) - v_k\|_{(H_k H_k^T)^{-1}}^2$ , minimization of  $\|e_{k,a}^+(\delta Q_k)\|^2$  corresponds to minimization of  $\|m_k(\delta Q_k)\|^2$  except for the term of  $v_k$ .

In the sense of minimization of estimation error covariance, we can consider the problem of minimizing  $E\{\|e_{k,a}^+(\delta Q_k)\|^2\}$ . However, in this article, we employ the problem of minimizing  $E\{\|m_k(\delta Q_k)\|_{R_k^{-1}}^2\}$  from the perspective of an adaptive filter based on the measurements. It should be noted that these problems are not equivalent because  $e_{k,a}^+(\delta Q_k)$  and  $m_k(\delta Q_k)$  contain  $v_k$  differently.

## APPENDIX B ACCUMULATION OF FICTITIOUS NOISE

In this appendix, we show by a simple example that fictitious noises with nonzero  $\beta_k$  accumulate in the estimation error covariance matrix  $P_k^+$  and cause large estimation errors when the measurement matrix  $H_k$  varies significantly. We consider the system where  $n = 2m$ ,  $F_i = I_{n \times n}$ ,  $Q_i = O_{n \times n}$  and  $R_i = R$  for all  $i$ , and suppose that  $H_i$  varies with  $i$ , but it satisfies  $H_i = (I_{m \times m}, O_{m \times m})$  for  $i = k, k+1, \dots, k+N$ .

We also assume that after the computation of EKF at time step  $k-1$ , the estimation error covariance  $P_{k-1}^+$  is block diagonal as

$$P_{k-1}^+ = \begin{pmatrix} P_{1,k-1}^+ & O_{m \times m} \\ O_{m \times m} & P_{2,k-1}^+ \end{pmatrix}.$$

At time step  $k$ , fictitious noise  $\delta Q_k$  is added to  $Q_k$  such that

$$\begin{aligned} \Delta P_k &= \alpha_k H_k^T R_k^{-1} H_k + \beta_k \mathcal{H}_k^\perp \\ &= \begin{pmatrix} \alpha_k \Lambda_k & O_{m \times m} \\ O_{m \times m} & \beta_k \Lambda_k^\perp \end{pmatrix}. \end{aligned}$$

Then,  $P_k^+(\delta Q_k)$  can be obtained from (21) by straightforward calculation as

$$\begin{aligned} P_k^+(\delta Q_k) &= \begin{pmatrix} P_{1,k}^+ & O_{m \times m} \\ O_{m \times m} & P_{2,k}^+ \end{pmatrix} \\ P_{1,k}^+ &= \left( I - P_{1,k-1}^+ (P_{1,k-1}^+ + R)^{-1} \right) P_{1,k-1}^+ + \alpha_k \Lambda_k \end{aligned} \quad (71)$$

$$P_{2,k}^+ = P_{2,k-1}^+ + \beta_k \Lambda_k^\perp. \quad (72)$$

Repeating (72) from time step  $k$  to time step  $k+N$ , we obtain

$$P_{2,k+N}^+ = P_{2,k-1}^+ + \sum_{i=k}^{k+N} \beta_i \Lambda_i^\perp. \quad (73)$$

From (73), we can see that  $\beta_i \Lambda_i^\perp$  caused from the fictitious noise accumulates in  $P_{2,k+N}^+$  without decreasing. It should be noted that, as  $N$  increases, the inflation of  $P_{2,k+N}^+$  becomes large unboundedly. On the other hand, from (71),  $P_{1,k}^+$  can be reduced from  $P_{1,k-1}^+$  through multiplying it by the gain  $(I - P_{1,k-1}^+ (P_{1,k-1}^+ + R)^{-1})$ . Although  $\alpha_k \Lambda_k$  is added in the right-hand side of (71), it can also be reduced at time step  $k+1$  in  $P_{1,k+1}^+$  by the gain  $(I - P_{1,k}^+ (P_{1,k}^+ + R)^{-1})$ .

Next, we assume that the measurement matrix changes at time step  $k + N + 1$  as  $H_{k+N+1} = (I_{m \times m}, I_{m \times m})$ . Then, the Kalman gain at time step  $k + N + 1$  can be calculated as

$$\begin{aligned} K_{k+N+1} &= \begin{pmatrix} P_{1,k+N}^+ (P_{1,k+N}^+ + P_{2,k+N}^+ + R)^{-1} \\ P_{2,k+N}^+ (P_{1,k+N}^+ + P_{2,k+N}^+ + R)^{-1} \end{pmatrix} \\ &\equiv \begin{pmatrix} K_1 \\ K_2 \end{pmatrix}. \end{aligned}$$

If  $P_{2,k+N}^+$  is very large due to the accumulation of  $\beta_i \Lambda_i^\perp$ ,  $K_1 \approx O_{m \times m}$  and  $K_2 \approx I_{m \times m}$ . Denoting  $\hat{x}_{k+N+1}^+$  as  $[\hat{x}_1^T, \hat{x}_2^T]^T$ ,  $\hat{x}_1$  would not be updated sufficiently according to the measurement innovation, because the Kalman gain  $K_1$  for  $\hat{x}_1$  is much smaller than it should be. On the other hand,  $\hat{x}_2$  would fluctuate greatly due to the measurement noise, because  $K_2$  for  $\hat{x}_2$  is too large. As a result, the accumulation of  $\beta_i \Lambda_i^\perp$  would lead to the degradation of filter performance.

It should be noted that the observability is guaranteed by the variation of  $H_k$ . However, since the observability is temporarily degenerate for  $i = k, k+1, \dots, k+N$ , the inflation of  $P_{2,i}^+$  due to  $\beta_i \Lambda_i^\perp$  cannot be suppressed. Too large inflation of  $P_{2,i}^+$  degrades the filter performance as mentioned above, at the time step when the measurement matrix changes. This measurement matrix change often happens for the systems working in unknown environments such as a mobile robot in Section IV and an automobile in Section V.

## REFERENCES

- [1] J. Zhang, M. Kaess, and S. Singh, "On degeneracy of optimization-based state estimation problems," in *Proc. IEEE Int. Conf. Robot. Autom. (ICRA)*, May 2016, pp. 809–816.
- [2] D. Tardioli and J. L. Villarroel, "Odometry-less localization in tunnel-like environments," in *Proc. IEEE Int. Conf. Auto. Robot Syst. Competitions (ICARSC)*, May 2014, pp. 65–72.
- [3] S. Thrun, W. Burgard, and D. Fox, *Probabilistic Robotics*. Cambridge, MA, USA: MIT Press, 2005.
- [4] S. Dan, *Optimal State Estimation: Kalman,  $H_\infty$ , and Nonlinear Approaches*. Hoboken, NJ, USA: Wiley, 2006.
- [5] Y. Takayama, T. Urakubo, and H. Tamaki, "Novel process noise model for GNSS Kalman filter based on sensitivity analysis of covariance with poor satellite geometry," *Sensors*, vol. 21, no. 18, p. 6056, Sep. 2021.
- [6] Y. Takayama, T. Urakubo, and H. Tamaki, "Avoiding GNSS Kalman filter degradation in urban canyons with a novel process noise model," in *Proc. 35th Int. Tech. Meeting Satell. Division Inst. Navigat. (ION GNSS)*, Oct. 2022, pp. 1831–1839.
- [7] G. Gawrys and V. Vadelinde, "Divergence and the fading memory filter," in *Proc. IEEE Conf. Decis. Control, 14th Symp. Adapt. Processes*, Dec. 1975, pp. 66–68.
- [8] G. Gawrys and V. Vadelinde, "On the steady-state error of the fading memory filter," *IEEE Trans. Autom. Control*, vol. AC-21, no. 4, pp. 624–625, Aug. 1976.
- [9] J. Sacks and H. Sorenson, "Nonlinear extensions of the fading memory filter," *IEEE Trans. Autom. Control*, vol. AC-16, no. 5, pp. 506–507, Oct. 1971.
- [10] R. Mehra, "On the identification of variances and adaptive Kalman filtering," *IEEE Trans. Autom. Control*, vol. AC-15, no. 2, pp. 175–184, Apr. 1970.
- [11] N. Stacey and S. D'Amico, "Adaptive and dynamically constrained process noise estimation for orbit determination," *IEEE Trans. Aerosp. Electron. Syst.*, vol. 57, no. 5, pp. 2920–2937, Oct. 2021.
- [12] C. Hide, T. Moore, and M. Smith, "Adaptive Kalman filtering algorithms for integrating GPS and low cost INS," in *Proc. Position Location Navigat. Symp. (PLANS)*, Apr. 2004, pp. 227–233.
- [13] J. O. A. L. Filho, E. L. F. Fortaleza, J. G. Silva, and M. C. M. de Campos, "Adaptive Kalman filtering for closed-loop systems based on the observation vector covariance," *Int. J. Control.*, vol. 95, no. 7, pp. 1731–1746, Jul. 2022.
- [14] R. Mehra, "Approaches to adaptive filtering," *IEEE Trans. Autom. Control*, vol. AC-17, no. 5, pp. 693–698, Oct. 1972.
- [15] B. Or and I. Klein, "A hybrid model and learning-based adaptive navigation filter," *IEEE Trans. Instrum. Meas.*, vol. 71, pp. 1–11, 2022.
- [16] F. Wu, H. Luo, H. Jia, F. Zhao, Y. Xiao, and X. Gao, "Predicting the noise covariance with a multitask learning model for Kalman filter-based GNSS/INS integrated navigation," *IEEE Trans. Instrum. Meas.*, vol. 70, pp. 1–13, 2021.
- [17] A. H. Jazwinski, *Stochastic Processes and Filtering Theory*. Cambridge, MA, USA: Academic Press, 1970.
- [18] R. Fitzgerald, "Divergence of the Kalman filter," *IEEE Trans. Autom. Control*, vol. AC-16, no. 6, pp. 736–747, Dec. 1971.
- [19] C. Harald, *Mathematical Methods of Statistics*. Princeton, NJ, USA: Princeton Univ. Press, 1946.
- [20] J. J. Spilker Jr., P. Axelrad, B. W. Parkinson, and P. Enge, *Global Positioning System: Theory and Applications*, vol. 1. Reston, VA, USA: American Institute of Aeronautics and Astronautics, 1996.
- [21] P. Groves, *Principles of GNSS, Inertial, and Multisensor Integrated Navigation Systems*, 2nd ed. Boston, MA, USA: Artech House, 2013.
- [22] D. Wang, Y. Dong, Z. Li, Q. Li, and J. Wu, "Constrained MEMS-based GNSS/INS tightly coupled system with robust Kalman filter for accurate land vehicular navigation," *IEEE Trans. Instrum. Meas.*, vol. 69, no. 7, pp. 5138–5148, Jul. 2020.
- [23] G. Dissanayake, S. Sukkarieh, E. Nebot, and H. Durrant-Whyte, "The aiding of a low-cost strapdown inertial measurement unit using vehicle model constraints for land vehicle applications," *IEEE Trans. Robot. Autom.*, vol. 17, no. 5, pp. 731–747, Oct. 2001.
- [24] T. Tominaga and N. Kubo, "Performance assessment of adaptive Kalman filter-based GNSS PVT and integrity in dense urban environment," *Trans. Navigat.*, vol. 4, no. 2, pp. 49–58, 2019.



**Yoji Takayama** received the B.E. and M.E. degrees from Doshisha University, Kyoto, Japan, in 2006 and 2008, respectively, and the Ph.D. degree in engineering from Kobe University, Kobe, Hyogo, Japan, in 2023.

He joined with Furuno Electric Company Ltd., Nishinomiya, Hyogo, in 2009, where he is currently a Chief Engineer. Since 2009, he has been mainly worked on the development of GNSS positioning algorithms and tightly coupled sensor fusion systems.



**Takateru Urakubo** (Member, IEEE) received the B.E., M.E., and Ph.D. degrees in aeronautics and astronautics from Kyoto University, Kyoto, Japan, in 1996, 1998, and 2001, respectively.

In 2001, he joined with Kobe University, Kobe, Japan, as an Assistant Professor, where he is currently an Associate Professor with the Graduate School of System Informatics. From 2007 to 2009, he was a Visiting Research Scientist at Carnegie Mellon University, Pittsburgh, PA, USA. His current research interests include nonlinear dynamical systems, nonlinear control theory, and autonomous robots.



**Hisashi Tamaki** (Member, IEEE) received the B.S., M.S., and Ph.D., degrees in electrical engineering from Kyoto University, Kyoto, Japan, in 1985, 1987, and 1993, respectively.

He is a Professor with the Graduate School of System Informatics, Kobe University, Kobe, Japan. His research interests include system optimization, emergent computation, and agent-based simulation.